

## Research Article

# Investigation of Control of Residual Stress Induced by CO<sub>2</sub> Laser-Based Damage Mitigation of Fused Silica Optics

**Chuanchao Zhang, Wei Liao, Lijuan Zhang, Yayun Ye, Jing Chen, Haijun Wang, Xiaoyu Luan, and Xiaodong Yuan**

*Research Center of Laser Fusion, China Academy of Engineering Physics, Mianyang 621900, China*

Correspondence should be addressed to Xiaodong Yuan; [yxd66my@163.com](mailto:yxd66my@163.com)

Received 27 February 2014; Accepted 11 May 2014; Published 3 June 2014

Academic Editor: Haiyan Xiao

Copyright © 2014 Chuanchao Zhang et al. This is an open access article distributed under the Creative Commons Attribution License, which permits unrestricted use, distribution, and reproduction in any medium, provided the original work is properly cited.

A CO<sub>2</sub> laser-based annealing technique for the mitigation of damaged sites of fused silica is studied to suppress the residual stress left on the surface. The laser annealing by a linear decrease of the CO<sub>2</sub> laser power effectively reduces the residual stress. The residual stress of mitigated sites is characterized by polarimetry, the reduction of the maximum retardance around the mitigated sites with the exposure time of laser annealing fits a stretched exponential equation, and the maximum retardance with optimal laser annealing is reduced ( $36 \pm 3$ )% compared to that without laser annealing. The residual stress regions are destructively characterized by introducing damage. The critical size of damage leading to fracture propagation for the mitigated sites without laser annealing is in the range of 120~230  $\mu\text{m}$ , and the corresponding critical size of damage for the mitigated sites with laser annealing is larger than 600  $\mu\text{m}$ . According to the relationship between maximum damage size and critical stress, the residual stress without laser annealing is in the range of 28–39 MPa and the residual stress with laser annealing is less than 17 MPa. These results indicate that the CO<sub>2</sub> laser-based annealing technique has a positive effect on the control of residual stress induced by CO<sub>2</sub> laser-based damage mitigation.

## 1. Introduction

For the high-power UV laser systems, fused silica materials are universally used to fabricate large aperture optics, such as windows, lenses, gratings, and debris shields, but one of the challenging issues for high-cost fused silica optics is laser-induced damages [1, 2]. Although the fabrication techniques of fused silica optics have been considerably improved, the damage precursors are still present as defects produced during the manufacturing process [3]. With a high-fluence irradiation, these precursors may be initiated as laser damage, and the damage will grow exponentially upon subsequent laser shots and will result in excessive light scattering and beam modulation, and finally it will lead to the failure of fused silica optics [4].

Various techniques including chemical etch, plasma etch, microflame torch, and CO<sub>2</sub> laser treatment have been developed to mitigate the growth of the surface damage, and the most successful method at this time is the CO<sub>2</sub> laser treatment to locally melt or evaporate the damage [5]. Upon the

working temperature and exposure time, there are two kinds of CO<sub>2</sub> laser-based mitigation approaches, evaporative and nonevaporative [6–10]. The nonevaporative approach works at lower temperature for longer time and uses longer pulses with lower peak power to heal the damaged material via some combination of material flow and thermal annealing. It has the advantage of minimal surface perturbation or material removal, no redeposited debris in or around the damage site, and just needs a simple system setup [8–10].

The nonevaporative approach has been successfully applied to damaged sites with lateral dimensions less than 110  $\mu\text{m}$  [8]. For the mitigation of larger damaged sites by nonevaporative technique, one of the limits is the residual stress, which may lead to that the cracks induced by the exposure of the CO<sub>2</sub> beam or the high-fluence UV laser propagate away from the mitigated damaged sites [6]. Therefore, an effective control of the residual stress to an acceptable level is necessary for the mitigation of larger damaged sites by the nonevaporative approach. Jiang et al. reported that the nonevaporative technique can be used to mitigate damaged sites with lateral

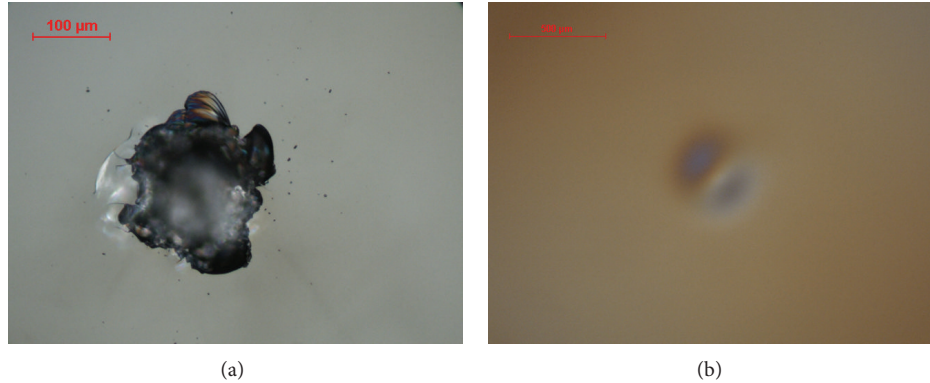


FIGURE 1: Typical micrographs of damage site before mitigation (a) and after mitigation (b) by  $\text{CO}_2$  laser.

sizes as large as  $400\ \mu\text{m}$ , but the high temperature annealing by using an oven must be applied to relieve the residual stress of the mitigated sites [11, 12].

In this paper, the nonevaporative approach is explored to mitigate the damaged sites as large as  $250\ \mu\text{m}$ , and the investigation of the  $\text{CO}_2$  laser-based annealing technique is conducted to suppress the residual stress left on the surface of fused silica optics for the mitigation of larger damaged sites by the nonevaporative approach.

## 2. Experimental Details

The samples used in this study are polished UV-grade Corning 7980 fused silica, 40 mm square and 4 mm thick. The fused silica samples were lightly etched in the buffered hydrofluoric (HF) acid solutions and then cleaned by deionized water. Damaged sites with lateral size of about  $250\ \mu\text{m}$  were created on the output surface of these blank samples by using a frequency-tripled Nd:YAG laser (Saga) operating at 355 nm, 6.3 ns with a  $1/e^2$  beam diameter of  $800\ \mu\text{m}$ . Generally, damaged sites with smaller lateral size were first initiated with higher laser fluence, and then subsequent laser shots with lower fluence were irradiated to increase the damage size to about  $250\ \mu\text{m}$ .

A commercial radio frequency power excited  $\text{CO}_2$  laser (Coherent GEM-100 L) with a maximum output power of 100 watt and power stability of  $\pm 3\%$  was used to mitigate the damaged sites of the fused silica samples. The spatial profile of the  $\text{CO}_2$  laser beam is Gaussian, and a beam spot with a diameter of 4.2 mm at  $1/e^2$  at the sample surface was obtained by a ZnSe lens with a 20 mm focal length for the mitigation of the damaged sites. For mitigating the damaged sites with diameter of  $250\ \mu\text{m}$ , the damaged sites were first preheated with low laser power of 13.7 watt for 30 seconds and then irradiated by high power of 25.3 watt for 4 seconds. To minimize the residual stress of the mitigated sites left on the surface of fused silica sample, a variety of linear decreases in power of the  $\text{CO}_2$  laser from 19.7 watt to 8.7 watt with different exposure times were performed following the mitigation.

The morphology of mitigated sites was measured using a Nikon-LV 100 optical microscope. The residual stress field of mitigated sites was characterized with a photoelastic tool

(PTC-702). The method is based on the property of birefringence under stress [13]. A critical damage size leading to fracture propagation due to residual stress was applied to precisely determine the amplitude of residual stress, and a series of damaged sites with different lateral size in the range from  $100\ \mu\text{m}$  to  $1400\ \mu\text{m}$  were introduced on the surface of the residual stress zones around the mitigated sites by the Nd:YAG laser operating at 355 nm.

Laser damage threshold measurements of the mitigated sites and pristine materials were performed with a frequency-tripled Nd:YAG laser (Saga), which delivers a pulse length of 6.3 ns at 355 nm with a diameter of  $800\ \mu\text{m}$  at  $1/e^2$  at the sample surface. The R-on-1 procedure was used to do damage testing. In the R-on-1 test, a variety of fluences gradually increased on each site, ten shots for each fluence, and the measurement was stopped when the first damage occurred. For each set of parameters, a series of sites were created and analyzed, and the results given in this study are based on a statistical analysis on the fused silica samples.

## 3. Results and Discussion

Figure 1 shows the typical micrographs of damage site before mitigation and after mitigation by  $\text{CO}_2$  laser. After mitigation, the damage site was effectively healed, and a central melt zone was observed at the mitigated site. Generally, the  $\text{CO}_2$  laser beam energy is intensively absorbed locally at the damage site of fused silica sample, and this induces a rapid temperature increase in the irradiation zone. Thermal expansion in the irradiated region occurs with increasing temperature. Because the irradiated region is surrounded by the other parts of the fused silica sample, the expansion of the heated material induces compressive stress in the irradiated region. As the material in the irradiated region heats up to a peak temperature exceeding the glass transition temperature, the material of damage site melted and healed, while the compressive stress in the melt zone is completely relaxed and the surrounding compressive stress decreases. After switching off the  $\text{CO}_2$  laser beam, a rapid thermal quench ensues. The melt zone of mitigated site can not completely relax the strained material over the time that is shorter compared to structural relaxation time, and a structure corresponding to high

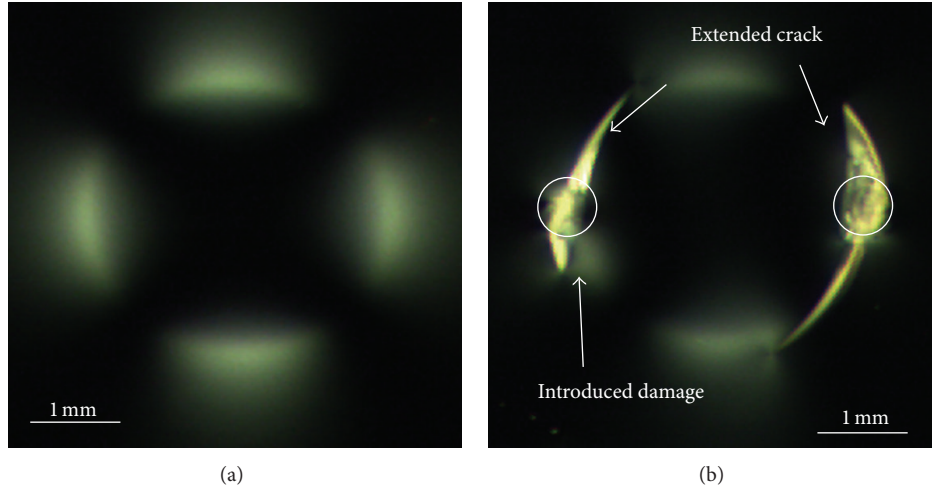


FIGURE 2: (a) A typical image of a mitigated site observed by a photoelastic tool (PTC-702). (b) A typical image of fracture extending for the introduced damage site at the location of the maximum retardance.

temperature is frozen at higher density, so the melt zone is plastically deformed. After collective cooling of the fused silica sample, the thermal expansion of the irradiated region vanishes and the plastic deformation of the melt zone with higher density remains, and the central melt zone undergoes tensile stress [14–16].

The residual stress distribution of the mitigated site is measured by a photoelastic tool (PTC-702). A light pattern associated to the stress distribution is observed, and a maximum of phase retardance was around the mitigated site as shown in Figure 2(a). According to the report of Gallais et al. [13], the location of the maximum retardance is vulnerable to damage initiation. And even worse, if a small damage site is introduced at the location of the maximum retardance, the residual stress may lead to that the cracks of the introduced damage site propagate away as shown in Figure 2(b), which causes a catastrophic failure of the fused silica optics. Thus, the residual stress around the mitigated site must be suppressed to avoid the destruction of the fused silica optics.

To effectively control the residual stress after damage mitigation, the region of plastic deformation should be clearly identified. The temperature distribution along the axis of the mitigated site can be steadily calculated using a steady-state approximation with the following equation [17]:

$$T_z(P, a, z) = \frac{(1-R)P}{2ak\sqrt{\pi}} \left(1 - \text{Erf}\left(\frac{z}{a}\right)\right) \exp\left(-\left(\frac{z}{a}\right)^2\right) + T_0, \quad (1)$$

where  $P$  is the  $\text{CO}_2$  laser power for damage mitigation,  $a$  is the  $1/e$  laser beam radius,  $k$  is the thermal conductivity,  $R$  is the reflectivity,  $T_z(P, a, z)$  is the temperature on the axis with depth  $z$  under the surface, and  $T_0$  is the ambient room temperature. Assuming  $1 - R = 0.85$ ,  $k = 0.02 \text{ W cm}^{-1} \text{ K}^{-1}$ ,  $a = 1.5 \text{ mm}$ , and  $P = 25.3 \text{ W}$ , the temperature distribution along the axis of the mitigated site was achieved. During the 4-second damage mitigation process, the fused silica materials at high temperatures with relaxation time constant less than 4 seconds have sufficient time to approach the equilibrium state

corresponding to the thermodynamic temperature. Upon quenching after switching off the  $\text{CO}_2$  laser, the structures of these materials at high temperatures are maintained at the states that they reached at high temperatures due to the extremely large cooling rate. According to the report of Zhao et al. [18], the relaxation time constant of fused silica is 4 seconds for a temperature of 1581 K, and according to the calculated result of the temperature distribution along the axis during mitigation process, the temperature of 1581 K locates at the depth  $z = 0.7 \text{ mm}$  under the surface. Therefore, the materials in the irradiated region on the axis as deep as 0.7 mm are plastically deformed after collective cooling of the fused silica sample.

If the cooling rate of the materials in the irradiated region after damage mitigation is effectively slowed, the structures of these materials that they reached high temperatures may gradually change to the states corresponding to low thermodynamic temperatures during the decrease of the temperature. Feit et al. reported [16] a linear ramp down of the  $\text{CO}_2$  laser power following the damage mitigation can effectively suppress the plastic deformation induced by the quenching, and the more gradual the cooling, the smaller the plastic deformation. A linear decrease of  $\text{CO}_2$  laser power from 19.7 watt to 8.7 watt with different exposure times was performed following the damage mitigation to minimize the residual stress. Figure 3 shows the change of maximum retardance around the mitigated sites resulting from identical heating but different exposure times of the linear ramp down of the  $\text{CO}_2$  laser power. The maximum retardance first decreases abruptly with the increase of the exposure time and then gradually changes to steady amplitude. A better fit to the experimental data of the maximum retardance with increasing exposure time was performed, and the equation can be written as

$$R(t) = R_0 + A \times \exp\left(-\left(\frac{t}{\tau}\right)^\beta\right), \quad (2)$$

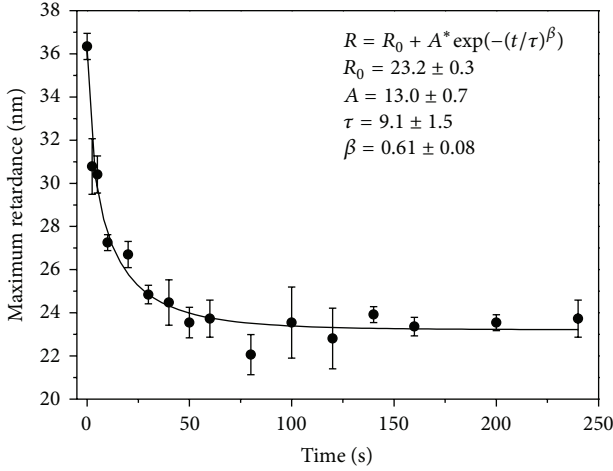


FIGURE 3: The maximum retardance measured around the mitigated site as a function of the exposure times of the linear ramp down of the CO<sub>2</sub> laser power.

where  $R(t)$  is the maximum retardance with exposure time  $t$  of the power ramp down,  $R_0 = (23.2 \pm 0.3)$  nm is the maximum retardance without exposure of the power ramp down,  $A = (13.0 \pm 0.7)$  nm is a time-independent constant,  $\tau = (9.1 \pm 1.5)$  s is the average relaxation time, and  $\beta = (0.61 \pm 0.08)$  is the stretched exponential parameter. This formation is consistent with the stretched exponential Kohlrausch-William-Watts function for the structural relaxation of glass reported by Scherer [19].

It is found that the maximum retardance with optimal exposure time of the CO<sub>2</sub> laser power linear ramp down is reduced ( $36 \pm 3$ )% as compared to that without exposure of the power ramp down. Thus, the residual stress around the mitigated sites is effectively suppressed by the CO<sub>2</sub> laser-based annealing with the power ramp down following the damage mitigation. If there is an exact relation between the retardance value and the residual stress level, we may precisely evaluate the change of the residual stress. But the retardance is integrated over the thickness of the irradiated region, and there is no direct proportionality between the maximum retardance value and the residual stress level. To precisely determine the amplitude of residual stress, a series of damaged sites with different lateral size in the range from  $100 \mu\text{m}$  to  $1400 \mu\text{m}$  were introduced on the locations of maximum retardance around the mitigated sites by Nd:YAG laser. If the diameter of the damage site is larger than the critical size, the residual stress will lead the fracture to extend. By statistically analyzing the size of the damaged sites that will propagate away due to the residual stress, the amplitude of the residual stress can be exactly determined by the following equation [15]:

$$\sigma_c = \frac{K_I}{\sqrt{\pi l}}, \quad (3)$$

where  $\sigma_c$  is the critical stress,  $K_I = 0.75 \text{ MPa m}^{1/2}$  is the fracture toughness of fused silica, and  $l$  is the maximum flaw length. The experimental results indicated that for mitigated

TABLE 1: Residual stress at the location of maximum retardance without or with laser annealing.

	Without annealing	With annealing
Residual stress (MPa)	$28 < \sigma_c < 39$	$\sigma_c < 17$

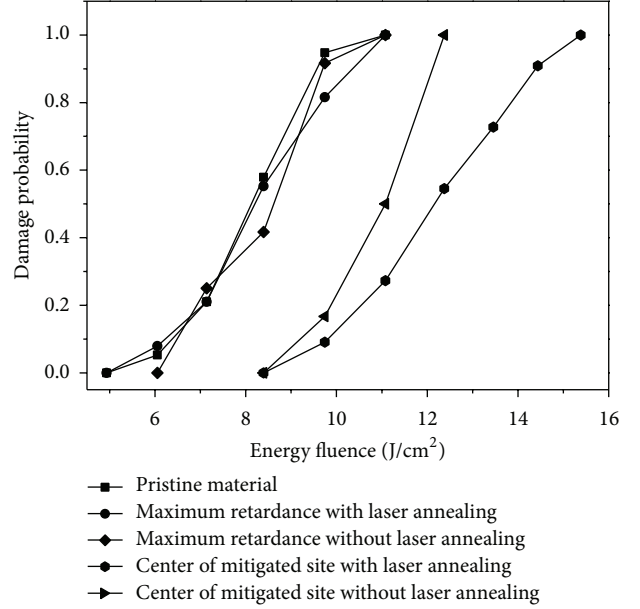


FIGURE 4: Damage threshold of pristine material and mitigated sites without and with laser annealing.

sites without CO<sub>2</sub> laser-based annealing the critical size of damage leading to fracture propagation for the mitigated sites is in the range of  $120 \sim 230 \mu\text{m}$  and that for mitigated sites with CO<sub>2</sub> laser-based annealing the corresponding critical size of damage is larger than  $600 \mu\text{m}$ . Calculated from (3), the residual stress without and with CO<sub>2</sub> laser-based annealing is obtained and shown in Table 1. It is found that the residual stress is reduced dramatically after laser annealing.

The CO<sub>2</sub> laser-based nonevaporative mitigation technique has been used to enhance the laser-induced damage threshold (LIDT), but the effect of laser annealing on the LIDT of mitigated sites is not clear. The LIDT of pristine material, mitigated sites without laser annealing, and mitigated sites with laser annealing were measured by Nd:YAG laser operating at  $355 \text{ nm}$  and  $6.3 \text{ ns}$ , and the results are shown in Figure 4. After laser annealing of mitigated sites, the LIDT in the center of the mitigated site is better than that without laser annealing and the LIDT of the 0% damage probability with laser annealing is even 60% more than that of pristine material. In addition, the LIDT at the location of maximum retardance around the mitigated site keeps the level of the pristine material. Thus, laser annealing after the CO<sub>2</sub> laser-based nonevaporative mitigation technique can effectively enhance the LIDT of damaged sites.

## 4. Conclusion

The CO<sub>2</sub> laser-based annealing technique for the nonevaporative mitigation of damaged sites as large as  $250 \mu\text{m}$  was



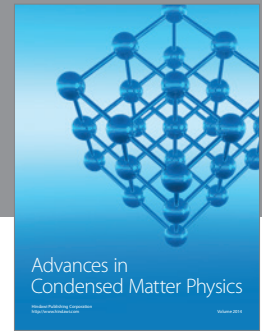
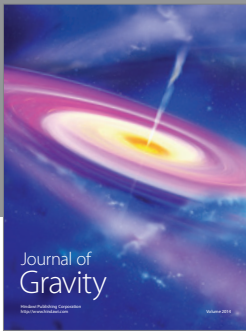
studied to limit the residual stress left in the surface of optics. The annealing parameters were systematically taken into account, and an annealing method by the linear decrease of the CO<sub>2</sub> laser power following the end of the nonevaporative mitigation effectively minimizes the residual stress. The residual stresses of mitigated sites were characterized by the photoelastic tool, and the change of the maximum retardance around the mitigated sites follows a stretched exponential equation, and the maximum retardance with optimal laser annealing is reduced ( $36 \pm 3$ )% compared to that without laser annealing. The destructive characterization of residual stresses by introducing a surface flaw to determine the critical size leading to fracture propagation was performed. The critical size is in the range of 120~230  $\mu\text{m}$  without laser annealing, and the corresponding critical size is larger than 600  $\mu\text{m}$  with laser annealing. According to the relationship of maximum damage size and critical stress, the residual stress is less than 17 MPa with laser annealing. The laser damage measurement indicated that laser annealing can effectively enhance the laser-induced damage threshold. These results provide sufficient evidence that the CO<sub>2</sub> laser-based annealing technique has a positive effect on the control of residual stress induced by CO<sub>2</sub> laser-based damage mitigation.

## Conflict of Interests

The authors declare that there is no conflict of interests regarding the publication of this paper.

## References

- [1] J. H. Campbell, R. A. Hawley-Fedder, C. J. Stolz et al., "NIF optical materials and fabrication technologies: an overview," in *Optical Engineering at the Lawrence Livermore National Laboratory II: The National Ignition Facility*, Proceedings of SPIE, pp. 84–101, January 2004.
- [2] C. W. Carr, J. D. Bude, and P. Demange, "Laser-supported solid-state absorption fronts in silica," *Physical Review B*, vol. 82, no. 18, Article ID 184304, 2010.
- [3] T. A. Laurence, J. D. Bude, N. Shen et al., "Metallic-like photoluminescence and absorption in fused silica surface flaws," *Applied Physics Letters*, vol. 94, no. 15, Article ID 151114, 2009.
- [4] M. A. Norton, J. J. Adams, C. W. Carr et al., "Growth of laser damage in fused silica: diameter to depth ratio," in *Laser-Induced Damage in Optical Materials*, vol. 6720 of *Proceedings of SPIE*, September 2007.
- [5] L. W. Hrubesh, M. A. Norton, W. A. Molander et al., "Methods for mitigating surface damage growth on NIF final optics," in *Laser-Induced Damage in Optical Materials*, vol. 7504 of *Proceedings of SPIE*, pp. 23–33, October 2001.
- [6] I. L. Bass, G. M. Guss, and R. P. Hackel, "Mitigation of laser damage growth in fused silica with a galvanometer scanned CO<sub>2</sub> laser," in *Laser-Induced Damage in Optical Materials*, vol. 5991 of *Proceedings of SPIE*, September 2005.
- [7] I. L. Bass, G. M. Guss, M. J. Nostrand, and P. J. Wegner, "An improved method of mitigating laser induced surface damage growth in fused silica using a rastered, pulsed CO<sub>2</sub> laser," in *Laser-Induced Damage in Optical Materials*, vol. 7842 of *Proceedings of SPIE*, September 2010.
- [8] J. J. Adams, M. Bolourchi, J. D. Bude, G. M. Guss, M. J. Matthews, and M. C. Nostrand, "Results of applying a non-evaporative mitigation technique to laser-initiated surface damage on fused-silica," in *Laser-Induced Damage in Optical Materials*, vol. 7842 of *Proceedings of SPIE*, September 2010.
- [9] S. Palmier, L. Gallais, M. Commandré et al., "Optimization of a laser mitigation process in damaged fused silica," *Applied Surface Science*, vol. 255, no. 10, pp. 5532–5536, 2009.
- [10] E. Mendez, K. M. Nowak, H. J. Baker, F. J. Villarreal, and D. R. Hall, "Localized CO<sub>2</sub> laser damage repair of fused silica optics," *Applied Optics*, vol. 45, no. 21, pp. 5358–5367, 2006.
- [11] Y. Jiang, C.-M. Liu, C.-S. Luo et al., "Mitigation of laser damage growth in fused silica by using a non-evaporative technique," *Chinese Physics B*, vol. 21, no. 5, Article ID 054216, 2012.
- [12] Y. Jiang, X. Xiang, C.-M. Liu et al., "Two localized CO<sub>2</sub> laser treatment methods for mitigation of UV damage growth in fused silica," *Chinese Physics B*, vol. 21, no. 6, Article ID 064219, 2012.
- [13] L. Gallais, P. Cormont, and J.-L. Rullier, "Investigation of stress induced by CO<sub>2</sub> laser processing of fused silica optics for laser damage growth mitigation," *Optics Express*, vol. 17, no. 26, pp. 23488–23501, 2009.
- [14] J. Dowden, *The Theory of Laser Materials Processing*, Springer, New York, NY, USA, 2009.
- [15] M. J. Matthews, J. S. Stolken, R. M. Vignes et al., "Residual stress and damage-induced critical fracture on CO<sub>2</sub> laser treated fused silica," in *Laser-Induced Damage in Optical Materials*, vol. 7504 of *Proceedings of SPIE*, 2009.
- [16] M. D. Feit, M. J. Matthews, T. F. Soules et al., "Densification and residual stress induced by CO<sub>2</sub> laser-based mitigation of SiO<sub>2</sub> surfaces," in *Laser-Induced Damage in Optical Materials*, vol. 7842 of *Proceedings of SPIE*, September 2010.
- [17] S. T. Yang, M. J. Matthews, S. Elhadji et al., "Comparing the use of mid-infrared versus far-infrared lasers for mitigating damage growth on fused silica," *Applied Optics*, vol. 49, no. 14, pp. 2606–2616, 2010.
- [18] J. Zhao, J. Sullivan, J. Zayac, and T. D. Bennett, "Structural modification of silica glass by laser scanning," *Journal of Applied Physics*, vol. 95, no. 10, pp. 5475–5482, 2004.
- [19] G. W. Scherer, "Theories of relaxation," *Journal of Non-Crystalline Solids*, vol. 123, no. 1–3, pp. 75–89, 1990.



**Hindawi**

Submit your manuscripts at  
<http://www.hindawi.com>

